Prediction of Cloud Droplet Number in a General Circulation Model

S. J. Ghan and L. R. Leung
Pacific Northwest National Laboratory
Richland, Washington

We have applied the Colorado State University (CSU) Regional Atmospheric Modeling System (RAMS) bulk cloud microphysics parameterization to the treatment of stratiform clouds in the National Center for Atmospheric Research Community Climate Model (CCM2). The CSU RAMS cloud microphysics parameterization predicts mass concentrations of cloud water, cloud ice, rain and snow, and number concentration of ice. To predict droplet number and its dependence on aerosols, we have introduced the droplet number conservation equation

$$\frac{\partial N_c}{\partial t} = -\nabla \cdot (N_c V) + N_{vc} - E_{cv} - A_{cr} - C_{cr} - C_{ci} - C_{cs} - F_{ci}$$

where E_{cv} represents droplet evaporation; A_{cr} is the droplet sink due to droplet coalescence; C_{cr}, C_{ci}, and C_{cs}, are sinks due to collection by rain, ice and snow; and F_{ci} is the sink due to droplet freezing to form ice crystals. Assuming all cloud droplets are formed as air flows into clouds, the droplet nucleation rate can be expressed as $N_{vc} = -\nabla \cdot N(V)$ where N equals the number nucleated for flow from clear air into cloud, and zero for flow out. For stratiform clouds, we neglect droplet formation on the sides of the cloud, but account for both resolved and turbulent transport of air into both the top and base of the cloud:

$$N_{vc} = \frac{1}{\Delta_z}\left[\int_o^{\infty} w_b \; N_n(w_b)p(w_b)dw_b - \int_{-\infty}^{-0} w_t \; N_n(w_t)p(w_t)dw_t\right]$$

where Δ_Z is the model layer thickness, w is the vertical velocity, p(w) is the subgrid probability distribution of w at cloud base (subscript b) and cloud top (subscript t). The number nucleated N_n is parameterized in terms of vertical velocity, radiative cooling, aerosol number concentration, size distribution, and composition (Ghan et al. 1993, 1995). Supersaturation forcing by cloud-top radiative cooling is accounted for by expressing the number nucleated in terms of

$$w^* \equiv w - \frac{c_p}{1 - c_p T/(\epsilon L)} \frac{Q_r}{g}$$

which follows from consideration of the supersaturation balance (Ghan et al. 1993).

The probability distribution of vertical velocity is parameterized in terms of the grid cell mean and subgrid variance of vertical velocity, assuming a normal distribution. The subgrid variance of vertical velocity is related to the turbulent kinetic energy predicted in the Pacific Northwest National Laboratory version of CCM2. Turbulent kinetic energy is predicted by the application of the Yamada and Mellor (1979) second-order turbulence closure (level 2.5) scheme. The integrations over the probability distributions are performed semi-numerically, taking advantage of asymptotic behavior to perform part of the integration analytically.

To test the prediction of cloud droplet number, we have performed two simulations in which the aerosol number concentration, size distribution, and composition are prescribed. In both simulations the aerosol is composed of ammonium sulfate with a log-normal size distribution with a number mode radius of 0.05 µm and a geometric standard deviation of 2. The aerosol number concentration is prescribed at 100 cm^{-3} in one simulation and 1000 cm^{-3} in the other, representative of marine and continental aerosol concentrations, respectively. The simulations were per-formed at T42 resolution for a period of thirty days, beginning September 1.

The two simulations yield substantially different droplet number concentrations. Figure 1 shows the frequency distribution of the simulated droplet number concentration (averaged over all times cloud water is present) for the two simulations. Note that a small fraction (5%) of the clouds have droplet number concentrations exceeding the aerosol number concentration; this physically unrealistic result is due to differences between the treatment of vertical diffusion of droplets from the cloud and the treatment of airflow into the cloud. The median droplet number concentrations in the two simulations are 24 and 127 cm^{-3}, for aerosol number concentrations of 100 and 1000 cm^{-3}, respectively. Thus, a ten-fold increase in aerosol number resulted in a five-fold increase in droplet number.

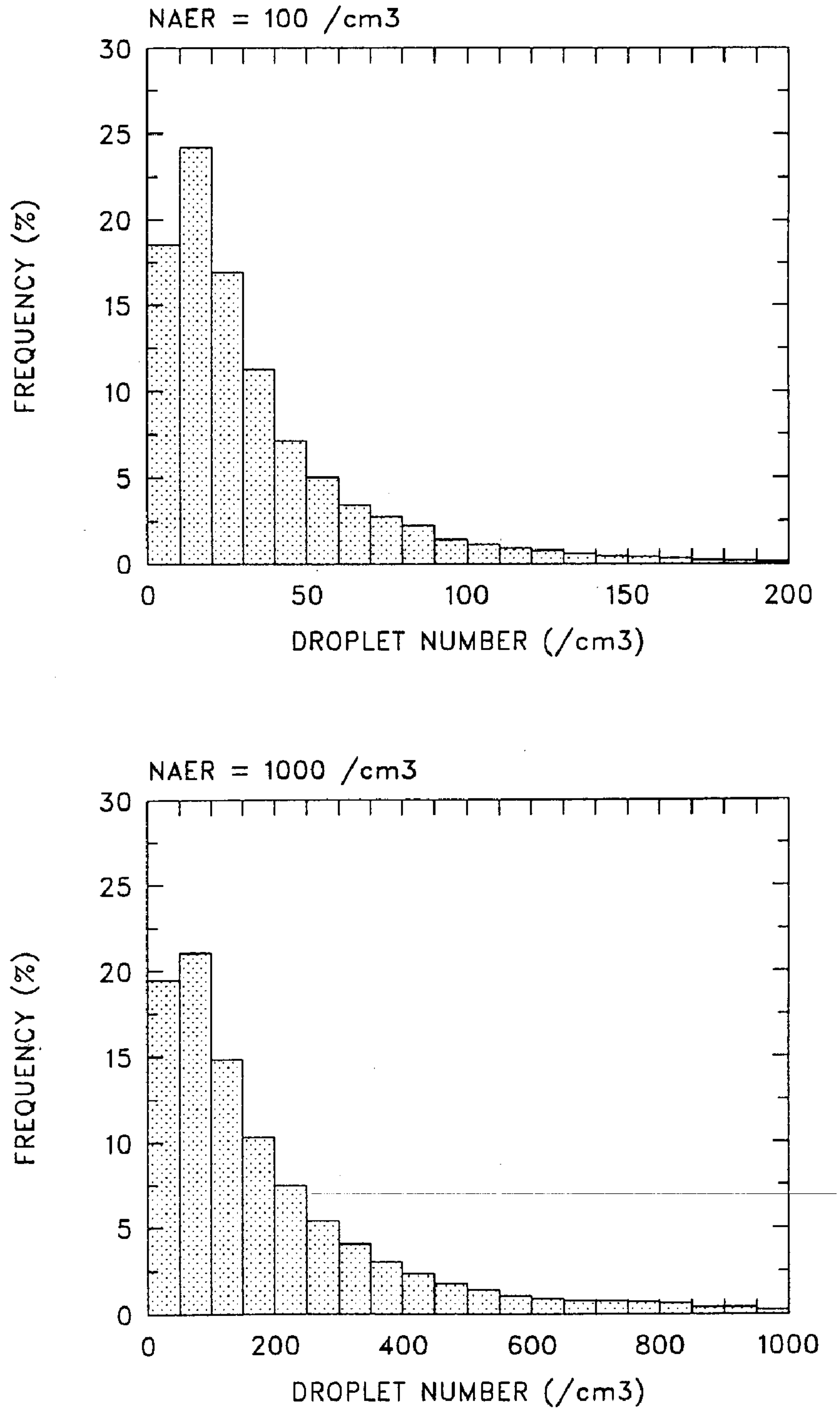

Figure 1. Frequency distribution of 30-day mean droplet number concentration simulated by Pacific Northwest National Laboratory version of CCM2 with aerosol number concentration prescribed at 100 cm^{-3} (above) and 1000 cm^{-3} (below).

The increased droplet number concentration resulted in an increase in the planetary albedo through two mechanisms. In addition to decreasing the effective radius of cloud droplets, increasing the droplet number concentration also permits higher cloud liquid water concentrations before autoconversion is initiated. The mean liquid water path of clouds is doubled by the increase in droplet number concentration. The mean cloud optical depth is more than doubled, partly due to the increase in liquid water path and partly due to the reduction in effective radius. The increase in the mean planetary albedo is 1.3%, corresponding to a 4.4 W m^{-2} increase in reflected solar radiation. We expect our estimate of the indirect radiative impact of aerosols to increase as we correct biases in the simulated low clouds and in the simulated partitioning between the liquid and ice phases of cloud water.

References

Ghan, S. J., C. C. Chuang, and J. E. Penner. 1993. A parameterization of cloud droplet nucleation. Part I: Single aerosol type, *Atmos. Res.*, **30**, 197-221.

Ghan, S. J., C. C. Chuang, R. C. Easter, and J. E. Penner. 1995. A parameterization of cloud droplet nucleation. Part II: Multiple aerosol types, *Atmos. Res.*, in press.

Yamada, T., and G. L. Mellor. 1979. A numerical simulation of BOMEX data using a turbulence closure model coupled with ensemble cloud relations, *Quart. J. Roy. Met. Soc.*, **105**, 915-944.